Reg Environ Change (2014) 14:75–89
DOI 10.1007/s10113-013-0435-5

ORIGINAL ARTICLE

Multitemporal analysis of cropland transition in a climate-sensitive area: a case study of the arid and semiarid region of northwest China

Lijun Zuo · Zengxiang Zhang · Xiaoli Zhao · Xiao Wang · Wenbin Wu · Ling Yi · Fang Liu

Received: 11 September 2012 / Accepted: 25 February 2013 / Published online: 12 March 2013

Abstract Land-use change is becoming an important anthropogenic force in the global climate system through alteration of the Earth's biogeophysical and biogeochemical processes. Cropland, which provides people with food, is the most variable vegetation land-use type and is affected by natural and anthropic forces and in turn affects the environment and climate system. This paper investigates the temporal-spatial pattern of cropland transition in the arid and semiarid region of northwest China, using remote sensing data for the late 1980s, 1995, 2000, 2005, 2008, and 2010. The aim was to clarify the change intensity and conversion pattern of cropland with a view to identifying the effects of a series of governmental policies and their influence on the climate system. Mathematical methodologies including the use of a transition matrix model, dynamic degree model, area-weighted centroid model, and area percentage were employed to analyze the temporal change in cropland. Meanwhile, a gridded zonal model with 10-km^2 resolution was used to detect the spatial pattern of cropland transition. During the period from the late 1980s to 2010, cropland increased dramatically by 23,182.17 km^2, an increase of 13.61 % relative to the area under cultivation in the late 1980s. Cropland transition accumulated in the western oasis–desert ecotone of the study area while it declined in the eastern farming–pastoral ecotone, leading to the westward movement of the cropland centroid. A net decrease in natural vegetation and unused land along with a net increase in built-up land due to cropland conversion was observed in the monitoring period. The three major driving forces of the cropland transition were population growth, economic development, and land-use management governed by the Grain for Green Program. The climate response to different conversion patterns was simply analyzed. However, quantitative assessment of the effect should be undertaken by employing ecosystem and climate models.

Keywords Cropland transition · Change intensity · Conversion pattern · Arid and semiarid region of northwest China · Driving forces · Climate response

L. Zuo · Z. Zhang (✉) · X. Zhao · X. Wang · L. Yi · F. Liu
Institute of Remote Sensing and Digital Earth,
Chinese Academy of Sciences, Beijing 100101, China
e-mail: zhangzx@irsa.ac.cn

W. Wu
Institute of Agricultural Resources and Regional Planning,
Chinese Academy of Agricultural Sciences,
Beijing 100081, China

Introduction

Cropland is a crucial land-use type, as it has enormous consequences for both environmental sustainability and food security (Audsley et al. 2006; Stehfest et al. 2007). It is estimated that almost 20 % of the potentially vegetated surface of the Earth was used for agriculture in 1992 (Ramankutty and Foley 1999; Ramankutty et al. 2002). Furthermore, as agricultural food production has doubled in the last 35 years of the twentieth century, another doubling is anticipated so as to meet the increasing human demands for food and fiber (Tilman 1999).

The arid and semiarid region of northwest China plays an important role in the food security of China, the world's most populous country, not only because of the plentiful land available for cultivation in this region (Dai et al. 2008), but also because of the lower economic cost of reclamation compared with that in southern China (Zhang et al. 2004). A large land resource including desert land and

grassland has been reclaimed for cropland since the 1980s. For instance, the proportion of China's reclaimed cropland accounted for by the municipality of Xinjiang and Inner Mongolia dramatically increased from 12.78 % in 1980 to 46.58 % in 1995 (Ren and Cai 1998; Cai and Guo 1999). However, because of the vulnerable environment and sensitive local climate system(Fang and Xie 2010), the increase in intensity of land reclamation has exacerbated originally serious environmental problems and initiated climate changes locally, regionally, and even globally.

Ta et al. (2006) revealed a strong relationship between the number of spring dust storms and the increase in area of annual land reclamation in the Tarim Basin and Hexi Corridor. A widely distributed fall in the groundwater level of between 3 and 5 m because of human activity was observed in the Shiyang River Basin in particular in the past 50 years (Ma et al. 2005). Desertification and salinization caused by cropland irrigation were recorded in northwest China (Wang 2000; Chen et al. 2010). Evidence of climate change caused by cropland transition was also observed. (Wang et al. 2011) found that conversion of freely grazed grassland to cropland, combined with overgrazing, led to an annual average decline of 2.3–2.8 % in the soil organic carbon of China, which would affect global warming. (Xu et al. 2007) detected an increase in air temperature in northwest China since 1995 caused by a decrease in vegetation coverage.

Numerous ecological problems and observed climate changes indicate the environmental degradation and climate sensitivity of northwest China. These effects have threatened the well-being of people living there (Kang et al. 2004; Ye and Van Ranst 2009). To contain these problems, the Chinese central government has implemented a series of environmental programs since the late 1990s (Dai 2010). The most renowned has been the Grain for Green Program, which called for cultivated land with slopes steeper than 25° to be gradually shifted to forest and grassland and restored with vegetation or changed into terraced land; accordingly, there was a shift of about 15 million ha of low-yield farmland to forest and grassland by 2010 (Feng et al. 2005). This unprecedented project resulted in another extensive cropland transition; it was reported that 7.19 million ha of low-yield cropland had been converted into forest and pasture land by 2003 (Xu et al. 2006).

Cropland in the arid and semiarid region of northwest China has obviously undergone profound change, initiating severe ecological problems and climatic alterations. Detailed assessments of impacts on the eco-environment and climate system require knowledge of the explicit dynamic patterns of cropland transitions. The purpose of the present research is to investigate the cropland transition patterns caused by anthropogenic activities from the late 1980s to 2010, which spans the period of extensive cropland reclamation and the implementation of a series of environmental policies. There are two aspects to the specific research objective: (1) analysis of the temporal dynamics and spatial differences in the intensity of cropland change, and of the conversion pattern on the basis of interpreted land-use and land-use change maps for the period from the late 1980s to 2010 in the study area; and (2) exploration of the interrelationship between cropland transition, socioeconomic development and policies, and the effects of cropland transition on the climate system.

Study area and data preparation

Study area

The arid and semiarid region of northwest China is a zone of the Physical Regionalization of China established by the National Agricultural Regionalization Committee (NARC 1984). It spans the vast area of 73°33′–121°3′E longitude and 36°32′–51°53′N latitude and accounts for almost all of the Inner Mongolia Autonomous Region, Xinjiang Uygur Autonomous Region, and Gansu Province, and the northern part of the Ningxia Hui Autonomous Region, Shaanxi Province, Shanxi Province, and Hebei Province (Fig. 1a). This region accounts for 29.8 % of the land area in China, while accounting for only 4.5 % of the country's population. Located in the mid-temperate zone and warm temperate zones, this area has a typical arid climate with strong solar radiation and long sunshine hours, little precipitation, and large variation in interannual precipitation.

According to the Integrated Agriculture Regionalization of China, the study area is divided into two agricultural zones, the region of Inner Mongolia and along the Great Wall in the east and the Gan-Xin region in the west (Fig. 1a). The eastern zone is a farming–pastoral ecotone with a vulnerable eco-environment. As the annual average precipitation is 200–400 mm and the frost-free period is 100–150 d, the cultivated land is single cropped in this region. The major cultivars include spring wheat, sorghum, millet, and potato. The western part is dominated by oasis cultivation and desert grazing and is referred to as an oasis–desert ecotone. An abundant heat resource and large diurnal temperature range are beneficial to crop growth; however, limited precipitation makes irrigation necessary for cultivation. Wheat and cotton are the major cultivars in this region.

Data preparation

A land-use dataset for the study area was acquired for cropland transition analysis. The dataset includes a land-use map of the study area for the late 1980s, 1995, 2000, 2005, 2008, and 2010 (Fig. 1b) and land-use change map for the periods of the late 1980s–2000, 1995–2000,

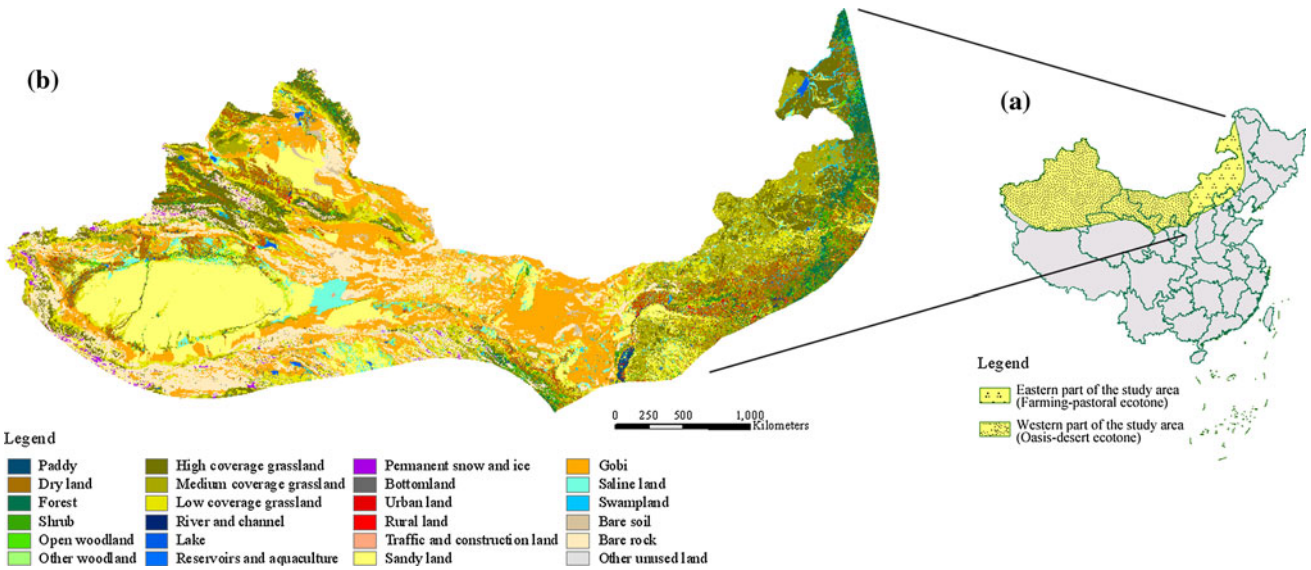

Fig. 1 Location of the study area (**a**) and a land-use map of the study area for 2010 (**b**)

2000–2005, 2005–2008, and 2008–2010. The maps are part of the China Land Use Dataset scaled at 1:100,000 established by the Chinese Academy of Sciences.

All land-use data in the China Land Use Dataset were visually interpreted by experts using remote sensing images mainly taken by Landsat TM/ETM+. Images obtained in crop-growing seasons (from June through September in the study area) with <10 % cloud coverage were selected. About 3,000 TM/ETM+ images were used in total, in which more than 300 images were for late 1980s, 421 for 1995, 508 for 2000, 412 for 2005, 488 for 2008, and 870 for 2010 (Zhang et al. 2012a, b). Photographic film and thousands of images from CBERS (China–Brazil Earth Resource Satellite) and HJ-1 (Small Satellite Constellation for Environment and Disaster Monitoring Forecasting) were adopted when TM/ETM+ were not available. They were also used to provide additional information on phenology. The spatial resolution of these images is between 19.5 m (CBERS) and 30 m (TM/ETM+ and HJ-1).

Visual interpretation conducted by experts was based on integrated analyses on the spectral reflectance, location, and shape of the objects. In addition, a series of auxiliary datasets, such as map of soil type, map of vegetations, topographic map, and information on regional planning, were employed to improve the precision of interpretation. Eight research groups from eight institutes of Chinese Academy of Sciences participated in this project. Each of them was located in different provinces and conducted the visual interpretation of land use in the region nearby the place where it is located.

Field survey was taken to assess the accuracy of land-use datasets, as well as to consolidate the experts' experience of land-use identification. As the first dataset, the field survey for dataset in 1995 was conducted based on the sampling of all land-use patches in all of the provinces except Tibet Autonomous Region and Taiwan. After that, field surveys were primarily conducted on the samples of land-use change patches in each period (Zhang et al. 2012a). According to the sampled field survey, the precision of land-use identification is higher than 90 % (Liu et al. 2003, 2010). The detailed information of the datasets' accuracy is given in Table 1 (Zhang et al. 2012a).

The classification system of this land-use dataset is hierarchical and has two levels. It includes six aggregated classes of land use: cropland, woodland, grassland, water, built-up land, and unused land. For subclasses, cropland is divided into paddy fields and dry farmland; woodland is divided into forest, shrubs, open woodland, and other; grassland is divided into high-coverage grassland, medium-coverage grassland, and low-coverage grassland; water is divided into rivers and channels, lakes, reservoirs and aquaculture, permanent snow and ice, tideland, and bottomland; built-up land is grouped into urban land, rural land, and traffic and construction land; and unused land is grouped into sandy land, Gobi, saline land, swampland, bare soil, bare rock, and other.

Methods

Models for temporal change analysis

Dynamic degree model and area-weight centroid for cropland change analysis

The temporal process of cropland change is determined using the dynamic degree model of cropland, which is

Table 1 Accuracy of land-use and land-use change datasets in each period

Period	Cropland	Woodland	Grassland	Built-up land	Water	Unused land	Total
1995							
Num	5,058	4,104	1,512	1,714	912		13,300
A (%)	94.94	90.13	88.16	96.32	95.72		92.92
1980s–2000							
Num	20,153	7,553	4,903	1,147	1,857	676	3,6289
A (%)	97.02	97.30	96.80	99.04	94.67	95.56	96.67
1995–2000							
Num	99,867	4,506	6,631	8,055	2561	1,526	33929
A (%)	99.09	98.92	97.96	98.92	96.86	97.88	98.04
2000–2005[a]							
Num	11,701	6,266	5,199	7,382	4056	1,392	35877
A (%)	99.30	97.75	98.62	97.01	97.61	98.28	98.56
2005–2008							
Num	4,235	9,584	2,073	7,589	2025	540	26046
A (%)	98.23	99.08	96.53	95.41	95.46	96.67	97.34
2008–2010							
Num	3,218	9,975	1,560	1,0872	2,194	296	2,7565
A (%)	98.94	97.36	98.59	96.44	95.92	97.64	97.15

Num number of verified patches, *A* accuracy

[a] the field survey of land-use change was conducted in seventeen provinces of China

developed from the dynamic change model of land use (Liu and Buheaosier 2000). It includes two parts: the net change degree S_n and total dynamic degree S_t. The two terms can be mathematically calculated according to

$$S_n = \frac{(\Delta A_{oc} - \Delta A_{co})}{(A_c \times t)} \times 100\,\%, \tag{1}$$

$$S_t = \frac{(\Delta A_{co} + \Delta A_{oc})}{(A_c \times t)} \times 100\,\%, \tag{2}$$

where A_c is the total area of cropland at the beginning of the monitoring period, ΔA_{co} is the area of cropland that is converted into other types of land use, ΔA_{oc} is the area of cropland involved in the opposite conversion, and t is the length of the period in units of years. The net change degree and total dynamic degree comprehensively represent the result and intensity of cropland dynamic change.

To investigate the temporal change in the cropland distribution, we employed an area-weight centroid model of cropland patches. The area-weighted centroids and the vectors linking the cropland centroids quantify the cropland distribution change in both distance and direction (Tang et al. 2012). Employing this method, we first calculated the locations of cropland centroids using the equations

$$X(t) = \frac{\sum_{i=1}^{n}(A_i(t) \times X_i(t))}{\sum_{i=1}^{n} A_i(t)}, Y(t) = \frac{\sum_{i=1}^{n}(A_i(t) \times Y_i(t))}{\sum_{i=1}^{n} A_i(t)}, \tag{3}$$

where $X(t)$ and $Y(t)$ are the area-weighted abscissa and ordinate of all the cropland patches in year t; $A_i(t)$ is the area of cropland patch i; n is the total number of patches of cropland; and $X_i(t)$ and $Y_i(t)$denote the abscissa and ordinate of cropland patch i. After determining the location of cropland centroids at different stages, the distance D and direction θ of the shift of centroids are defined as

$$\mathrm{D} = \sqrt{(X(t_2) - X(t_1))^2 + (Y(t_2) - Y(t_1))^2}, \tag{4}$$

$$\theta = \begin{cases} \arctan\left(\frac{Y(t_2)-Y(t_1)}{X(t_2)-X(t_1)}\right) if\ X(t_2) \geq X(t_1) \\ \pi - \arctan\left(\frac{Y(t_2)-Y(t_1)}{X(t_2)-X(t_1)}\right) if\ X(t_2) \leq X(t_1) \end{cases}, \tag{5}$$

where t_1 is the beginning of the monitoring period, and t_2 is the end of the monitoring period.

Transition matrix and area-percentage method for the analysis of conversion between cropland and other land-use types

The use of a transition matrix is a useful technique for analyzing observed land-use changes, by identifying the direction and magnitude of land-use transformations. These aspects of change are important in understanding the causes of land-use changes and in analyzing the effects of

these changes on the eco-environment and climate system (Macleod and Congalton 1998; Pérez-Hugalde et al. 2011). Here, we used three attributes of the coverage file of the land-use change map for the calculation of transition matrixes of the five periods; the attributes were the class codes of the transformation patch at the beginning and end of the period, and the area of the patch. These three attributes were exported as.dbf files in ArcGIS software. Cross-tabulation tables were then calculated using the PivotTable Wizard in Microsoft Excel and output as transition matrixes.

The area-percentage method was adopted to explore the structure of land-use classes as the source of newly emerging cropland and the structure of the target land-use classes into which cropland is converted. The contribution of one land-use class to the increase in area of cropland, *CR,* and the contribution of one land-use class to the lost area of cropland, *OP,* are, respectively, defined as

$$CR = \frac{A_{jc}}{A_{ci}}, \tag{6}$$

$$OP = \frac{A_{ck}}{A_{cl}}, \tag{7}$$

where A_{jc} denotes the area converted from land-use class j to cropland; A_{ci} denotes the total newly emerged area of cropland; A_{ck} denotes the area converted from cropland to land-use class k; and A_{cl} denotes the total area of lost cropland. The interclass difference and temporal change of *CR* and *OP* give convenient and explicit insight into the driving forces of cropland change.

A zonal model with 10-km^2 resolution for spatial difference analysis

To detect and represent the spatial difference in cropland changes, a gridded zonal model with resolution of 10 km^2 was established. The model produces a visible spatial distribution map of the cropland dynamic metrics with spatial resolution of 10 km^2, from which spatial patterns of cropland change can be designated. This kind of method has been widely used in the analysis of spatial and temporal characteristics of land-use change in China (Wang et al. 2010).

Four 10-km^2 gridded zonal products were obtained, namely the annual net area change for cropland, annual dynamic area of cropland, major land-use class converted into cropland, and major land-use class into which cropland was converted. First, we extracted cropland-related dynamic patches from the land-use change map. Second, we generated a standard grid frame in vector format using the FISHNET module in ArcGIS software in the scope of the study area. Each cell of the grid is 10 km by 10 km. Finally, we used the 10-km^2 grid to intersect with the cropland-related dynamic patches and obtain the four types of 10-km^2 gridded zonal products.

Results

Brief description of land-use and land-use change in the arid and semiarid region of northwest China

In the study area, the dominant land-use classes were unused land and grassland, accounting for 87.02 % of the region in 2010. Their areas were 1,571,314.03 and 932,250.21 km^2, respectively, in 2010 (Table 2). As indicated in Fig. 1b, the unused land, mainly composed of Gobi and sandy land, was largely distributed in the western oasis–desert ecotone. This indicates the arid characteristics of this zone. Cropland was the third largest land-use class, accounting for 6.73 % of the region, and was mainly located in water-abundant areas such as alluvial plains (the Tumochuan Plain and Hetao Plain) and foothills (the edge of the Junggar Basin, the Tarim Basin, and the Hexi Corridor of Gansu). Owing to the scarcity of water resources, dry land was the primary subclass of cropland in this region, accounting for about 97.18 % of the total area of cropland. Built-up land was usually scattered within the cropland, having an area of 18,347.55 km^2 in 2010 and was the smallest of the six land-use classes. Forest, accounting

Table 2 Changes in area for each land-use type from the late 1980s to 2010

Class	Total area (km^2)						Change rate in the period late 1980s–2010 (%)
	Late 1980s	1995	2000	2005	2008	2010	
Cropland	170,366.08	173,281.96	178,667.44	186,617.81	189,673.47	193,548.25	13.61
Forest	122,402.12	120,194.29	120,096.84	120,445.79	120,539.79	120,398.15	−1.64
Grassland	954,086.32	954,099.08	943,982.38	935,356.09	935,203.91	932,250.21	−2.29
Water	40,533.39	40,373.13	41,732.53	41,454.64	41,044.71	41,035.46	1.24
Built-up land	14,814.51	14,971.83	15,767.63	16,952.49	17,507.55	18,347.55	23.85
Unused land	1,574,691.23	1,573,973.36	1,576,646.83	1,576,066.83	1,572,924.22	1,571,314.03	−0.21

Table 3 Change intensity for cropland in each period from the late 1980s to 2010

Period	1980s–2000	1995–2000	2000–2005	2005–2008	2008–2010	2000–2010
Net change degree (%/year)	0.37	0.62	0.89	0.55	1.02	0.83
Total dynamic degree (%/year)	0.97	1.66	1.70	0.81	1.49	1.42

for 4.25 % of the region, lay mainly along the eastern edge of the region, where there is transition between semiarid and moist areas. The area of water was relatively small in the region, being just 41,035.46 km^2 in 2010. Permanent snow and ice, lakes, and bottomland accounted for 83.92 % of the total water area.

Over the past 20 years, land use in the study area underwent a remarkable change, especially in the case of built-up land and cropland, which increased in area by 23.85 and 13.61 %, respectively, from the late 1980s to 2010 (Table 2). Cropland, as an artificial vegetation type in the land-use classification system, was the only vegetation type that increased in area; the two natural vegetation types, forest and grassland, respectively, decreased in area by 1.64 and 2.29 % in the monitoring period. The increase in area of artificial landscapes including built-up land and cropland, along with the loss of natural landscapes such as forest and grassland, reveals the intensifying human disturbance of the eco-environment.

Analysis of cropland change intensity

Temporal changes of cropland change intensity

The total area of cropland continually increased in the monitoring period, with basically ascending net change degree (Table 3). The net change degree increased from 0.37 % per year from late 1980s to 2000 to 0.89 % per year in 2000–2005 and then decreased to 0.55 % per year in 2005–2008, before finally peaking at 1.02 % in 2008–2010. The temporal change trend of the total dynamic degree was similar with that of the net change degree, but peaked at different stage. The total dynamic degree continually increased in the first three periods and peaked in 2000–2005 at 1.70 % per year. It then decreased in 2005–2008 and increased again in 2008–2010 to 1.49 % per year. This indicates that the human disturbance of cropland was most intense in 2000–2005. The extensive policies implemented for economic development and eco-environment protection at the beginning of the new century in northwest China such as the "Go-West" Enterprise and Grain for Green Program might explain the frequent cropland transformation.

Spatial variation in cropland change intensity

The cropland change intensity varied in different stages and had distinct characteristics in the two agricultural zones as indicated in Fig. 2 and Table 4. The number of cells for which the net area of cropland increased and the number of cells for which the net area of cropland decreased in the eastern farming–pastoral ecotone were both slightly greater than the numbers for the western oasis–desert ecotone in the period from late 1980s to 2000 (Fig. 2a). As a result, a similar rate of net area increase was observed in the two ecotones (343.32 and 295.39 km^2/year, respectively) (Table 4). Cells in which the net area increased were mainly located where cropland was the dominant landscape, such as in the western foothills of the Daxianling Mountains, the Hetao Plain, the Hexi Corridor, and on the edges of the Junggar Basin (Fig. 2a). Many of these cells had a rate of net area increase >0.25 km^2/year. The cells with a net area decrease were mostly distributed in the transition area between cropland and other land-use types. Less suitable conditions (such as a lack of irrigation facilities) for farming in these places meant that cropland was easily abandoned. Most of these cells had a rate of net area decrease of <0.25 km^2/year. The number of cells for which the net area of cropland increased in the period 1995–2000 (Fig. 2b) was greater than that in the period from late 1980s to 2000, most of which had a rate of net area increase of faster than 0.50 km^2/y. It indicated that the net area of cropland decreased in the period from late 1980s to 1995 for these cells.

Entering the twenty-first century, the cells with a net area increase became concentrated in the western oasis–desert ecotone, while the cells with a net area decrease were mostly distributed in the eastern farming–pastoral ecotone (Fig. 2c, e). In the western oasis–desert ecotone,

Table 4 Change intensity of cropland in the eastern farming–pastoral ecotone and western oasis–desert ecotone from the late 1980s to 2010

Period	Net area change (km^2/year)		Total dynamic area (km^2/year)	
	East part	West part	East part	West part
1980s–2000	295.39	343.32	855.19	795.69
1995–2000	296.96	780.14	956.02	1924.11
2000–2005	−14.51	1604.58	807.20	2229.47
2005–2008	35.88	982.67	236.95	1282.11
2008–2010	−66.64	2004.03	176.77	2643.59
2000–2010	−9.82	1497.90	510.04	2028.09

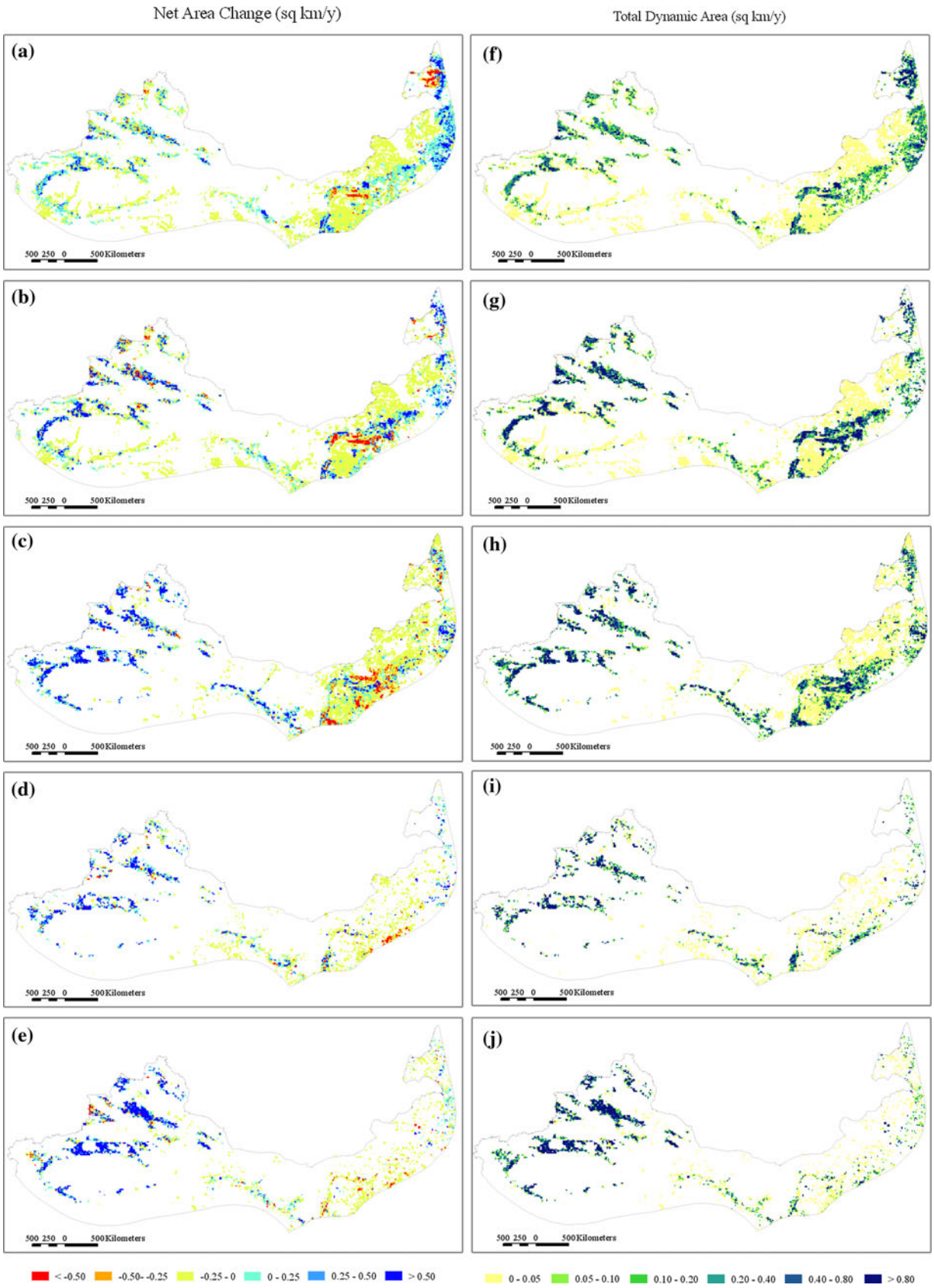

Fig. 2 Spatial distribution of net area change [(**a**) late 1980s–2000 (**b**) 1995–2000 (**c**) 2000–2005 (**d**) 2005–2008 (**e**) 2008–2010) and total dynamic area [(**f**) late 1980s–2000 (**g**) 1995–2000 (**h**) 2000–2005 (**i**) 2005–2008 (**j**) 2008–2010) of cropland within a 10-km^2 cell in each period

cells with a net area increase were dominant after 2000, resulting in an increase in total cropland area of 1497.90 km^2/year in the period 2000–2010, which was 4.36 times that in the period from the late 1980s to 2000. Meanwhile, in the eastern farming–pastoral ecotone, the number and intensity level of the cells with a net area increase (Fig. 2c, e) continued to decline after 2000 and the total cropland area decreased at a rate of 9.82 km^2/year in 2000–2012. The loss of cropland was most intense in Erdos and Baotou in the municipality of Inner Mongolia and Yanchi in the municipality of Ningxia (Fig. 2c, e). Urbanization, industrialization, and the implementation of ecological protection policy led to the distinct loss of cropland in these areas.

The cells with total dynamic area larger than 0.1 km^2/year also shifted from the eastern farming–pastoral ecotone to the western oasis–desert ecotone, while the opposite shift occurred in the cells with total dynamic area <0.1 km^2/year (Fig. 2f–i), indicating the intensified human interference on cropland in the west. In the period from the late 1980s to 2000, the annual total dynamic areas of the two ecotones were similar (855.19 km^2/year for the eastern part and 795.69 km^2/year for the western part) (Table 4). After 2000, the annual total dynamic area of the eastern farming–pastoral ecotone gradually declined to 177.67 km^2/year in 2008–2010. However, the situation in the western oasis–desert ecotone was the opposite; the annual total dynamic area of cropland climbed to 2643.59 km^2/year in 2008–2010. That is to say, the distribution of the human disturbance of cropland shifted from being evenly distributed in the study area to being concentrated in the west.

Centroid shift of cropland

The area-weighted centroid method was used to represent the spatial movement of cropland from the late 1980s to 2010 in the study area. Figure 3 shows the distance and direction of the shift of cropland. To improve the comparability of the movement, we omitted the centroid for 2008 so as to obtain the movement of centroids in the same length of period. The moving trend in the two stages before 2000 was basically motion in opposite directions, switching from a northeast direction at 34.15 degrees in the late 1980s to 1995 to a southwest direction at 142.14 degrees in 1995–2000. The distances of motion in these two periods were similar (9546.05 and 12,215.31 km, respectively). In the two stages after 2000, the centroid of cropland moved in a similar direction at about 280 degrees to the northwest, with the distance increasing from 63,923.65 to 83,385.01 km. This indicates that the imbalance of the cropland change between the eastern farming–pastoral ecotone and western oasis–desert ecotone increased as time passed.

Analysis of the cropland conversion pattern

To facilitate the analysis of cropland transitions, we grouped the dominant cropland conversion forms into three types: conversion with natural vegetation, conversion with built-up land, and conversion with unused land (cropland abandonment and unused-land reclamation). As the conversion between cropland and water only accounted for 0.26 % of the total dynamic area of cropland, it was ignored in this paper. Figures 4 and 5 show the temporal change and spatial difference of each kind of conversion, respectively.

Pattern of Conversion between cropland and natural vegetation

Conversion between cropland and natural vegetation, especially conversion between cropland and grassland, was the main type of cropland transformation in the study area. The annual area that was converted from grassland to cropland was between 790.42 km^2/year in 2005–2008 and 1896.07 km^2/year in 2008–2010 (Fig. 4b), which was much larger than areas for other land-use classes that converted into cropland. *CR* values of grassland in all

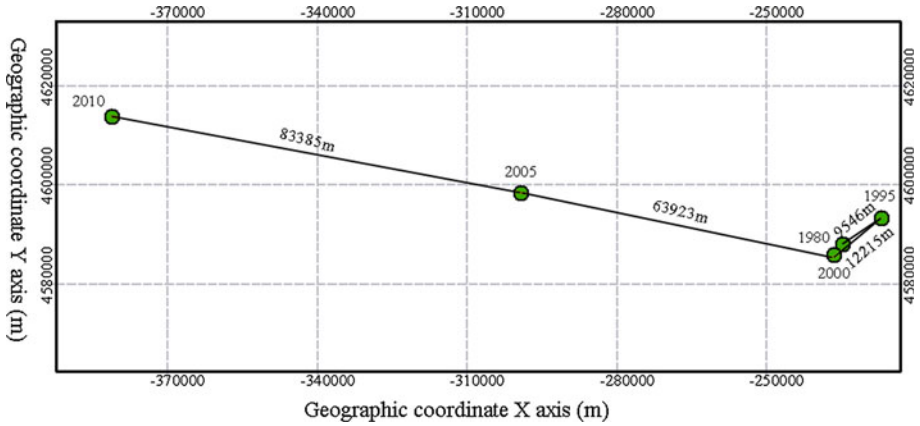

Fig. 3 Spatial movement of the area-weighted centroid of cropland from the late 1980s to 2010

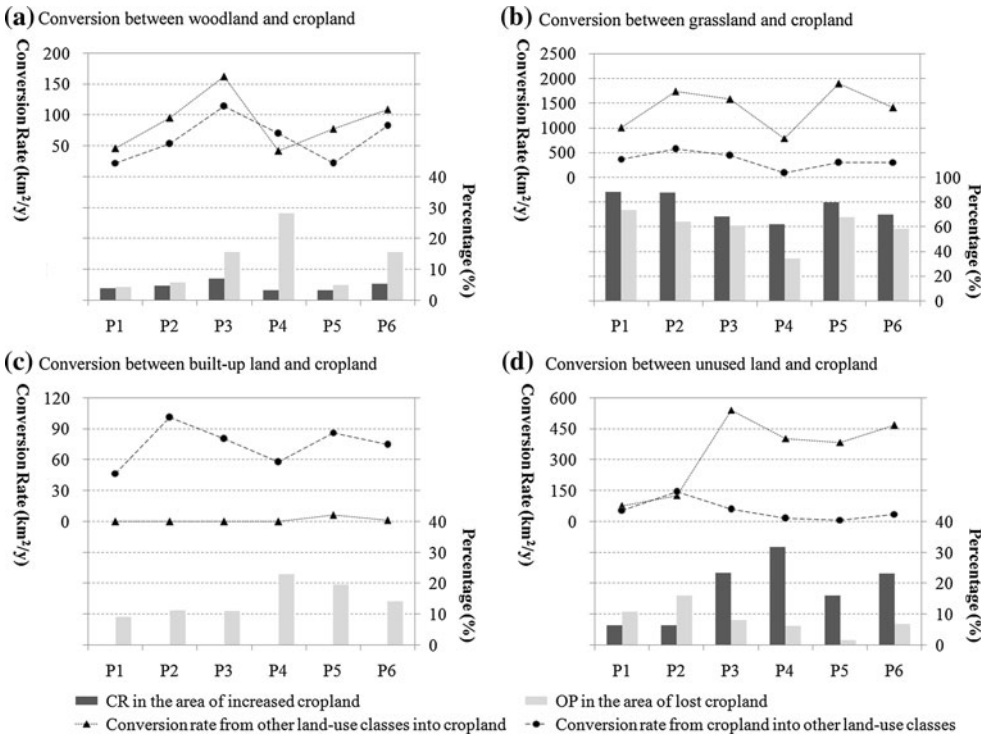

Fig. 4 Conversion rate of each kind of transformation and CR and OP in the area of increased and lost cropland (*P1*: late 1980s–2000, *P2*: 1995–2000, *P3*: 2000–2005, *P4*: 2005–2008, *P5*: 2008–2010, *P6*: 2000–2010)

stages were higher than 50 %, indicating that grassland was the major source of the newly emerged cropland. However, the decreasing trend of *CR* revealed the mitigated reclamation of grassland for cropland.

Cells with grassland as the primary source of the increase in cropland were evenly distributed in the study area at the beginning of the monitoring period (Fig. 5a). After 2000, the distribution of cells of this kind became concentrated in the western oasis–desert ecotone, and there were dramatically fewer grids of this kind in the eastern farming–pastoral ecotone. As a result, the area of grassland that was converted into cropland in the eastern farming–pastoral ecotone declined to 81.85 km^2 per year in 2008–2010, which was 2.21 % of that in the western oasis–desert ecotone.

The annual increase in area of grassland because of conversion from cropland in 2000–2010 was slightly less than that from the late 1980s to 2000. The number of cells with grassland as the major land-use class into which cropland was converted increased in the western oasis–desert ecotone and decreased in the eastern farming–pastoral ecotone (Fig. 5f–j).

The area that was converted from cropland to grassland was smaller than that involved in the opposite conversion in all stages; hence, there was a net increase in cropland in the exchange of grassland and cropland. It was also found that the proportion of high-coverage grassland in the area of lost grassland decreased from 303.80 km^2/year in the period from the late 1980s to 2000 to 129.04 km^2/year in 2008–2010, while that of low-coverage grassland dramatically increased from 214.22 to 1007.79 km^2/year (Table 5).

Similar to the case for grassland, the conversion between woodland and cropland resulted in a net increase in cropland in all periods except for 2005–2008 (Fig. 4a); hence, there was a decrease in natural vegetation and increase in cropland in the study area. However, *OP* for woodland in the area of lost cropland basically increased in the monitoring period, except during 2008–2010. Additionally, although the entire area of woodland decreased in the monitoring period, the areas of detected forest and other forest (generally including orchards, nurseries, and immature forest) increased by 25.15 and 52.72 km^2/year, respectively, in 2000–2010 (Table 6). This suggests that government policies, such as the Grain for Green Program and the Project of the Green Wall of China, were effective.

Pattern of conversion between cropland and built-up land

There was a remarkable expansion of built-up land throughout the country due to population growth and economic development. In the study area, there was serious appropriation of cropland for construction in the monitoring period as the area of conversion from cropland to built-up land increased slightly from 46.72 km^2/year in the

Table 5 Net rate of loss of grassland and its subclasses to cropland

Subclass	Net loss rate (km^2/year)					
	Late 1980s–2000	1995–2000	2000–2005	2005–2008	2008–2010	2000–2010
High-coverage grassland	303.80	396.00	225.43	140.20	129.04	180.58
Medium-coverage grassland	118.27	307.41	432.54	172.35	389.40	345.86
Low-coverage grassland	214.22	455.89	485.67	391.63	1077.79	575.88
Total	636.30	1159.29	1143.64	704.17	1596.22	1102.32

Table 6 Net rate of loss of woodland and its subclasses to cropland

Subclass	Net loss rate (km^2/year)					
	Late 1980s–2000	1995–2000	2000–2005	2005–2008	2008–2010	2000–2010
Forest	7.51	35.60	−45.20	12.90	7.15	−17.30
Shrub	9.12	6.90	64.80	16.85	9.28	39.31
Open woodland	6.48	10.56	34.88	9.11	17.31	23.64
Other forest	0.45	−11.34	−6.49	−67.51	21.28	−19.24
Total	23.55	41.72	48.00	−28.65	55.02	26.41

period of the late 1980s to 2000 to 74.79 km^2/year in the period 2000–2010 (Fig. 4c). *OP* for built-up land in the area of lost cropland had an increasing trend from 9.23 to 14.24 % in these two periods. As represented in Fig. 5g–j, the cells with built-up land as the major type into which cropland was converted were primarily located in the western oasis–desert ecotone before 2000. After 2000, this kind of cell was concentrated in the eastern farming–pastoral ecotone and mainly distributed on the Hetao Plain and Tumochuan Plain, where the population was large and cropland was of good quality.

Pattern of cropland abandonment and unused-land reclamation

The phenomenon of abandoning cropland was prevalent in northwest China, especially in the case of farming land without irrigation facilities. This adversely affects not only food security but also the eco-environment. However, the opposite transformation, the reclamation of unused land for cropland, could increase the area of cultivated land while mitigating the appropriation of natural vegetation for farming, leaving the ecological impact for further discussion. Monitoring showed that the area of reclaimed unused-land exceeded that of abandoned cropland (Fig. 4d). Additionally, there was a notable increase in *CR* for unused land before 2008, together with a decrease in *OP* for unused land. This demonstrates an exacerbated loss of unused land to cropland. As indicated in Fig. 5a–e, the reclamation of cropland from unused land was concentrated near oases in Gansu and the municipality of Xinjiang.

Discussion

Social, economic, and political factors of cropland transition

Socioeconomic factors, land-use management, and the natural environment are proposed as the three main driving forces of land-use/cover change (Turner et al. 1995). Population growth has been the basic driving force of change relating to cropland, a land-use type that provides people with food. Since the 1950s, the rapid population growth in China has meant that the supply of farm products has been insufficient for the whole country, and this encouraged the undertaking of a national survey to find more cultivable land (Tang et al. 2012). The arid and semiarid region of northwest China was delineated as a place with vast reserves of land for farming (Feng and Li 2000). For decades, cropland reclamation in this region has played an important role in realizing the balance of the requisition–compensation of cropland throughout the country. As found in this research, cropland basically expanded throughout the monitoring period at an increasing rate, especially on the edge of the Junggar Basin and Tarim Basin.

Economic development, along with urbanization and industrialization, was other important anthropogenic factors for cropland transition. In 2000, the national government promoted the "Go-West" Enterprise, which induced the remarkable economic development of northwest China. Large infrastructure comprising railways, highways, economic development zones, and industrial parks was constructed in this area. This phenomenon was embodied in

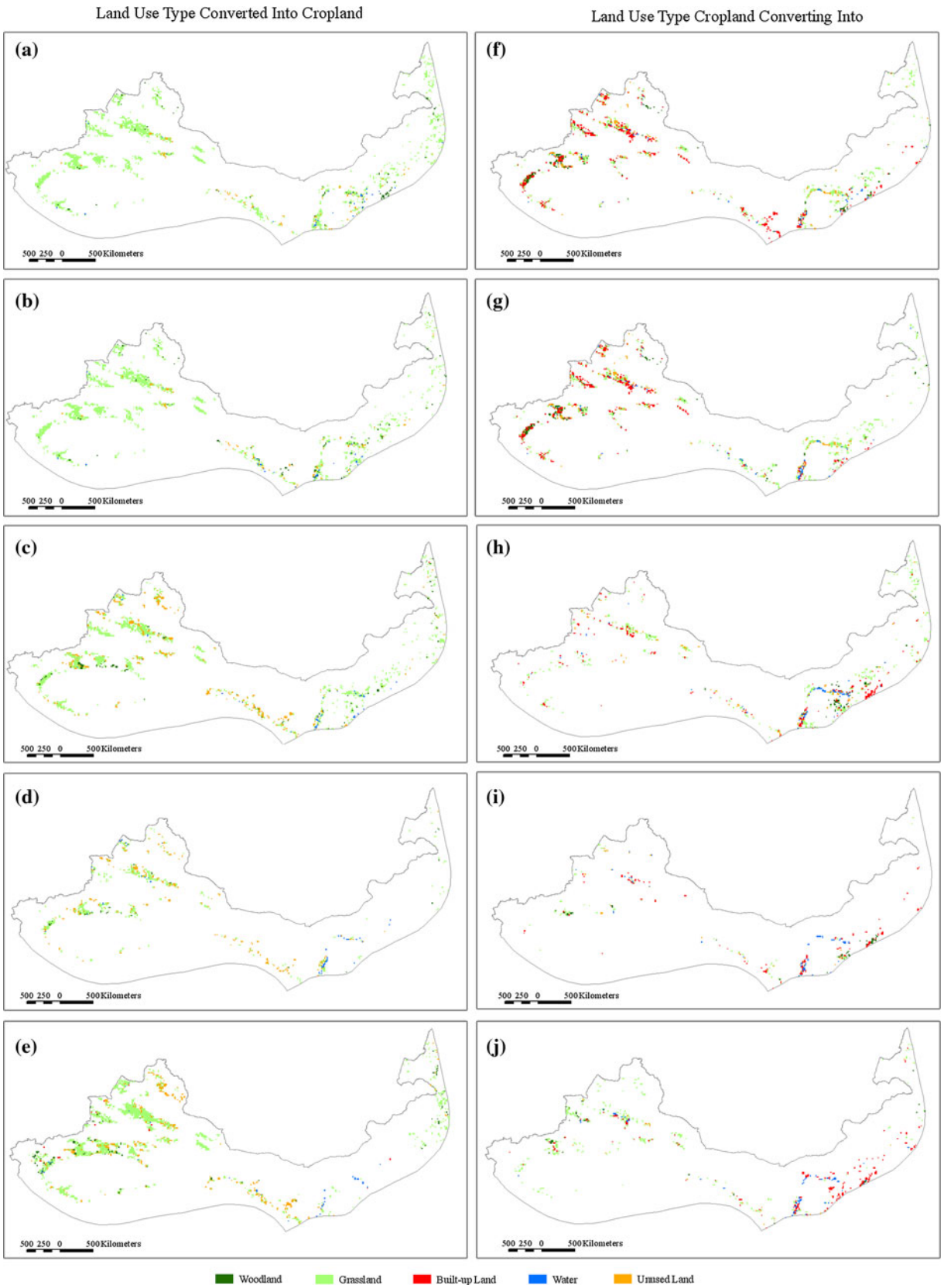

Fig. 5 Spatial distribution of the majority of land-use classes converted into cropland [(**a**) late 1980s–2000 (**b**) 1995–2000 (**c**) 2000–2005 (**d**) 2005–2008 (**e**) 2008–2010] and into which cropland converted [(**f**) late 1980s–2000 (**g**) 1995–2000 (**h**) 2000–2005 (**i**) 2005–2008 (**j**) 2008–2010] within a 10-km^2 cell in each period

the present research as the built-up land, which greatly expanded by 2579.92 km^2 (Table 2) in the period 2000–2010, a rate of expansion that was 2.7 times that in the period from the late 1980s to 2000. Of the newly emerged built-up land, 65.57 % came from appropriating cropland from the late 1980s to 2000. Although the proportion declined to 28.65 % in 2000–2010, cropland was still one of the major sources for the expansion of built-up land.

Another significant cause of cropland transition was land-use management governed by a series of eco-environment protection policies. The great effects came from the Grain for Green Program. This program was tested in pilot areas in 1999 and then implemented in 25 provinces in 2002. The implementation of the project directly induced tremendous transition between cropland and other vegetation types. It was reported that 66.86 million ha of cropland had been converted to forest in Gansu Province by 2008. In Inner Mongolia, there had been conversion of 92.2 million ha by 2010. As observed in this research, the total area of conversion from cropland to woodland was 8.26 million ha. The proportion of woodland in the area of lost cropland increased from 4.45 % before 2000 to 15.73 % after 2000 (Fig. 4a), and the increasing area of forest and other forest converted from cropland in 2000–2010 (Table 6) represents the effects of this policy on cropland transitions.

Effects of cropland transition on the climate system

Cropland-related transformation was the dominant type of land-use change in the arid and semiarid region of northwest China, accounting for 56.17 % of the entire area of land-use change. As a result, numerous climate changes caused by land-use alteration are supposed to result from the cropland transition. The climatic response to the conversion between cropland and other land-use classes is complicated. For one thing, cropland transitions affect biogeophysical processes that directly affect the local climate system. The current climate and vegetation coexist in a dynamic equilibrium that could be altered by large perturbations in either of the two components (Nobre et al. 1991). Cropland transition would largely modify the land surface parameters and thus alter the surface–atmosphere interaction, which would in turn affect the overlying atmosphere and thus the local climate (Sen et al. 2004; Lin et al. 2009). Both rainfall (Zheng et al. 2002) and surface temperature (Potter et al. 1981) would change. Furthermore, cropland transitions affect biogeochemistry processes, resulting in carbon emission and sequestration and thereby lead to changes to the concentration of carbon dioxide and the global climate system.

The effects of cropland transition on the climate system have been demonstrated in many research works. For effects on biogeophysical processes, Tinker (Tinker et al. 1996) found that rainfall may decrease where there is deforestation (including transformation from forest to cropland) in large continuous areas, and Lewis (Lewis 1998) announced that the ground surface temperature would increase in the temperate climate zone at the time of deforestation. The encroachment of cropland by built-up land enlarges the area of the impervious surface without vegetation cover and leads to a modified thermal climate that is much warmer than that in the surrounding area, which is known as the urban heat island effect (Giannaros and Melas 2012).

For the effects on biogeochemistry processes, the replacement of forest with cropland would radically reduce the soil carbon stocks, and a greater stock reduction has been found for cereal monoculture than for grasses (Karhu et al. 2011). An apparent loss of soil carbon stock has been observed after pasture conversion to cropland (Detwiler 1986; Davidson and Ackerman 1993; Wu et al. 2003). Xu et al. (2011) conducted a research on the soil organic carbon (SOC) change after the conversion of natural desert vegetation to oasis agriculture in northwest China. Results showed that there was a rapid augmentation of SOC in the first several years, followed by a fluctuation of SOC because of the change in cropland management.

Conclusions

The arid and semiarid region of northwest China, a climate-sensitive and eco-environment vulnerable area, has undergone profound land-use change in recent decades, especially in terms of cropland change, because of population growth and economic development. This study acquired land-use and land-use change information for this region from remote sensing data to analyze the temporal and spatial patterns of cropland transition from the late 1980s to 2010. Social, economic, and political factors of cropland transition and their effects on the climate system were then discussed. The main conclusions are as follows.

Over the past 20 years or so, the area of cropland in the study area dramatically increased by 23,182.17 km^2, which is an increase of 13.61 % relative to the area in the late 1980s. The net increase degree in the five investigated periods basically continually increased except in 2005–2008. The highest total dynamic degree occurred in 2000–2005, indicating the intense anthropogenic disturbance of cropland in this period because of the launch of extensive policies for economic development and eco-environment protection at the beginning of the twenty-first century. In the 10-km^2 gridded zoning of cropland change intensity, the distribution of cells with a net increase in cropland area and the distribution of cells with a large total

dynamic area both shifted from being evenly scattered throughout the whole study area to being concentrated in the western oasis–desert ecotone. The centroid of cropland also moved westward in the monitoring periods. This demonstrates that intense human interference became increasingly concentrated in the western oasis–desert ecotone, which is a more arid area.

Cropland conversion was grouped into three types: conversion with natural vegetation, conversion with built-up land, and conversion with unused land. Both conversion with natural vegetation and conversion with unused land resulted in a net increase in cropland, while the conversion with built-up land led to a net loss of cropland. Conversion with grassland, a subtype of conversion with natural vegetation, was the major transformation type of cropland transition. This kind of conversion basically reduced the area of grassland at an increasing rate and with an increasing proportion of low-coverage grassland, indicating that conversion between cropland and grassland shifted to the more vulnerable environment. The spatial dynamic of this conversion coincided with that of cropland change intensity. The conversion between cropland and woodland, another type of conversion with natural vegetation, resulted in a net area decrease in all subclasses before 2000; however, a net increase in two subclasses (i.e., forest and other forests) was detected after 2000. This suggests that government policies, such as the Grain for Green Program and the Project of the Green Wall of China, took effect. In the conversion with built-up land, the appropriation of cropland for building construction became serious in the monitoring period and declined in the western oasis–desert ecotone while accumulating in the eastern farming–pastoral ecotone. Conversion with unused land mainly occurred in the western oasis–desert ecotone.

The three major driving forces of the cropland transition were population growth, economic development, and land-use management governed by the Grain for Green Program. The effect of cropland transition on the climate system was complicated, as different kinds of conversion had different effects on the local and global climate. A quantitative assessment of the climate response to cropland transition should be undertaken by employing ecosystem models and climate models. For example, the dynamic land ecosystem model (DLEM) (Zhang et al. 2007; Tian et al. 2010) could be adopted to measure ET, heat transformation between land and atmosphere, as well as the changes on carbon stock. Regional climate model (RCM) (Giorgi and Shields 1999; Ju et al. 2007; Sylla et al. 2010) and general circulation model (GCM) (Joshi et al. 2003; Willett et al. 2010) could also be coupled to assess the changes of temperature and rainfall.

Our current research only emphasizes the temporal and spatial patterns, simply driving forces, and general effects on the climate system of cropland transition. This research can be further improved by identifying spatial explicit distribution of the patches where a conversion between cropland and other land-use types occurred in one period while the inverse conversion occurred in the following period. This kind of information is very helpful when effects on ecological environment and the climate system are intended to be evaluated. Another way to improve the exploration of cropland transition is redefining the classification of cropland to make it more practical for analyzing internal transitions of cropland. Dividing cropland into non-irrigated cropland and irrigated cropland would be more suitable in northwest China, as irrigation plays an important role in agriculture of northwest China. It would also be essential to investigate the agricultural intensification and assess its impacts on salinizaiton. Finally, generating land-use change datasets in the consecutive periods with fixed length is also anticipated to draw more convictive conclusions.

Acknowledgments This work was Supported by the National Program on Key Basic Research Project (973 Program) "Impact of Large-scale Land Use/Cover on Global Climate Changes" (2010CB95090102) and the National Natural Science Foundation of China (General Program) "Quantitative Assessment of Utilization Efficiency of Agricultural Land Coupling Remote Sensing Data and Econometrics Model" (41001277). The authors also express appreciation to Pro. Yan Changzhen from Cold and Arid Regions Environmental and Engineering Research Institute CAS, Pro. Wu Shixin from Xinjiang Institute of Ecology and Geography CAS, Pro. Zhang Shuwen from Northeast Institute of Geography and Agroecology CAS, Pro. Bao Yuhai from Inner Mongolia Normal University, and Pro. Xu Xinliang from Institute of Geographic Sciences and Natural Resources Research CAS for the contribution to the establishment of the land-use dataset used in this paper.

References

Audsley E, Pearn KR, Simota C, Cojocaru G, Koutsidou E, Rounsevell MDA, Trnka M, Alexandrov V (2006) What can scenario modelling tell us about future European scale agricultural land use, and what not? Environ Sci Policy 9(2):148–162

Cai Y, Guo H (1999) Evaluation and propose of exploitation of reserved cultivated land in the northern China. Prog Geogr 18(1):76–80 in Chinese

Chen W, Hou Z, Wu L, Liang Y, Wei C (2010) Evaluating salinity distribution in soil irrigated with saline water in arid regions of northwest China. Agric Water Manag 97(12):2001–2008

Dai Z (2010) Intensive agropastoralism: dryland degradation, the Grain-to-Green program and islands of sustainability in the Mu Us Sandy Land of China. Agric Ecosyst Environ 138(3–4):249–256

Dai B, Gu x, Chen B (2008) GIS-based suitability evaluation of uncultivated arable land in Xinjiang Region. Trans CSAE 24(7):60–64 in Chinese

Davidson EA, Ackerman IL (1993) Changes in soil carbon inventories following cultivation of previously untilled soils. Biogeochemistry 20(3):161–193

Detwiler R (1986) Land use change and the global carbon cycle: the role of tropical soils. Biogeochemistry 2(1):67–93

Fang CL, Xie Y (2010) Sustainable urban development in water-constrained Northwest China: a case study along the mid-section of silk-road–He-Xi corridor. J Arid Environ 74(1):140–148

Feng Z, Li X (2000) The stratagem of cultivated land and food supplies security: storing food in land-raising the comprehensive productivity of land resource of China. Geogr Terri Res 16(3): 1–5

Feng Z, Yang Y, Zhang Y, Zhang P, Li Y (2005) Grain-for-green policy and its impacts on grain supply in West China. Land Use Policy 22(4):301–312

Giannaros TM, Melas D (2012) Study of the urban heat island in a coastal Mediterranean City: the case study of Thessaloniki, Greece. Atmos Res 118:103–120 in Progress

Giorgi F, Shields C (1999) Tests of precipitation parameterizations available in latest version of NCAR regional climate model (RegCM) over continental United States. J Geophys Res 104(6):6353–6375

Joshi M, Shine K, Ponater M, Stuber N, Sausen R, Li L (2003) A comparison of climate response to different radiative forcings in three general circulation models: towards an improved metric of climate change. Clim Dyn 20(7):843–854

Ju L, Wang H, Jiang D (2007) Simulation of the last glacial maximum climate over East Asia with a regional climate model nested in a general circulation model. Palaeogeogr Palaeoclimatol Palaeoecol 248(3):376–390

Kang E, Li X, Zhang J, Hu X (2004) Water resources relating to desertification in the Hexi Area of Gansu Province. J Glaciol Geocryol 26(6):657–667 in Chinese

Karhu K, Wall A, Vanhala P, Liski J, Esala M, Regina K (2011) Effects of afforestation and deforestation on boreal soil carbon stocks—comparison of measured C stocks with Yasso07 model results. Geoderma 164(1–2):33–45

Lewis T (1998) The effect of deforestation on ground surface temperatures. Global Planet Change 18(1–2):1–13

Lin W, Zhang L, Du D, Yang L, Lin H, Zhang Y, Li J (2009) Quantification of land use/land cover changes in Pearl River Delta and its impact on regional climate in summer using numerical modeling. Reg Environ Change 9(2):75–82

Liu J, Buheaosier B (2000) Study on spatial-temporal feature of modern land use change in China: using remote sensing techniques. Quat Sci 20(3):228–238

Liu J, Liu M, Zhuang D, Zhang Z, Deng X (2003) Study on spatial pattern of land-use change in China during 1995–2000. Sci China Series D Earth Sci 46(4):373–384

Liu J, Zhang Z, Xu X, Kuang W, Zhou W, Zhang S, Li R, Yan C, Yu D, Wu S, Jiang N (2010) Spatial patterns and driving forces of land use change in China during the early 21st century. J Geogr Sci 20(4):483–494

Ma JZ, Wang XS, Edmunds WM (2005) The characteristics of ground-water resources and their changes under the impacts of human activity in the arid Northwest China—a case study of the Shiyang River Basin. J Arid Environ 61(2):277–295

Macleod RD, Congalton RG (1998) A quantitative comparison of change-detection algorithms for monitoring eelgrass from remotely sensed data. Photogramm Eng Remote Sensing 64(3):207–216

Nobre CA, Sellers PJ, Shukla J (1991) Amazonian deforestation and regional climate change. J Clim 4(10):957–988

Pérez-Hugalde C, Romero-Calcerrada R, Delgado-Pérez P, Novillo CJ (2011) Understanding land cover change in a special protection area in central Spain through the enhanced land cover transition matrix and a related new approach. J Environ Manag 92(4):1128–1137

Potter GL, Ellsaesser HW, MacCracken MC, Ellis JS (1981) Albedo change by man: test of climatic effects. Nature 291(5810):47–49

Ramankutty N, Foley JA (1999) Estimating historical changes in land cover: north American croplands from 1850 to 1992. Global Ecol Biogeogr 8(5):381–396

Ramankutty N, Foley JA, Norman J, McSweeney K (2002) The global distribution of cultivable lands: current patterns and sensitivity to possible climate change. Global Ecol Biogeogr 11(5):377–392

RC NA (1984) China natural regionalization summary. Science Press, Beijng

Ren G, Cai Y (1998) The characteristics and countermeasures related to exploitation of reserved cultivated land resources in China. Resour Sci 20(5):46–51 in Chinese

Sen OL, Wang B, Wang Y (2004) Impacts of re-greening the desertified lands in northwestern China: implications from a regional climate model experiment. J Meteorol Soc Jpn 82(6):1679–1693

Stehfest E, Heistermann M, Priess JA, Ojima DS, Alcamo J (2007) Simulation of global crop production with the ecosystem model Day cent. Ecol Model 209(2–4):203–219

Sylla MB, Coppola E, Mariotti L, Giorgi F, Ruti P, Dell'Aquila A, Bi X (2010) Multiyear simulation of the African climate using a regional climate model (RegCM3) with the high resolution ERA-interim reanalysis. Clim Dyn 35(1):231–247

Ta W, Dong Z, Sanzhi C (2006) Effect of the 1950s large-scale migration for land reclamation on spring dust storms in Northwest China. Atmos Environ 40(30):5815–5823

Tang J, Bu K, Yang J, Zhang S, Chang L (2012) Multitemporal analysis of forest fragmentation in the upstream region of the Nenjiang River Basin, Northeast China. Ecol Indic 23:597–607

Tian H, Chen G, Liu M, Zhang C, Sun G, Lu C, Xu X, Ren W, Pan S, Chappelka A (2010) Model estimates of net primary productivity, evapotranspiration, and water use efficiency in the terrestrial ecosystems of the southern United States during 1895–2007. Forest Ecol Manag 259(7):1311–1327

Tilman D (1999) Global environmental impacts of agricultural expansion: the need for sustainable and efficient practices. Proc Natl Acad Sci USA 96(11):5995–6000

Tinker PB, Ingram JSI, Struwe S (1996) Effects of slash-and-burn agriculture and deforestation on climate change. Agric Ecosyst Environ 58(1):13–22

Turner BL, David S, Liu Y. (1995) Land use and land cover changes science/research plan. IHDP Report, no. 07

Wang T (2000) Land use and sandy desertification in the north china. J Desert Res 20(2):103–107

Wang S-Y, Liu J-S, Ma T-B (2010) Dynamics and changes in spatial patterns of land use in Yellow River Basin. China Land Use Policy 27(2):313–323

Wang S, Wilkes A, Zhang Z, Chang X, Lang R, Wang Y, Niu H (2011) Management and land use change effects on soil carbon in northern China's grasslands: a synthesis. Agric Ecosyst Environ 142(3–4):329–340

Willett KM, Jones PD, Thorne PW, Gillett NP (2010) A comparison of large scale changes in surface humidity over land in observations and CMIP3 general circulation models. Environ Res Lett 5(2):025210

Wu H, Guo Z, Peng C (2003) Land use induced changes of organic carbon storage in soils of China. Global Change Biol 9(3): 305–315

Xu Z, Xu J, Deng X, Huang J, Uchida E, Rozelle S (2006) Grain for Green versus Grain: conflict between food security and conservation set-aside in China. World Dev 34(1):130–148

Xu X, Zhang F, Levy J (2007) The influence of land surface changes on regional climate in Northwest China. Adv Atmos Sci 24(3):527–537

Xu W, Chen X, Luo G, Lin Q (2011) Using the CENTURY model to assess the impact of land reclamation and management practices

in oasis agriculture on the dynamics of soil organic carbon in the arid region of North-western China. Ecol Complex 8(1):30–37

Ye L, Van Ranst E (2009) Production scenarios and the effect of soil degradation on long-term food security in China. Global Environ Change 19(4):464–481

Zhang D, Zhang F, An P, Liu L (2004) Potential economic supply of uncultivated arable land in China. Res Sci 26(5):46–52 in Chinese

Zhang C, Tian H, Chappelka AH, Ren W, Chen H, Pan S, Liu M, Styers DM, Chen G, Wang Y (2007) Impacts of climatic and atmospheric changes on carbon dynamics in the Great Smoky Mountains National Park. Environ Pollut 149(3):336–347

Zhang Z, Zhao X, Wang X (2012a) Remote sensing of land use in China. Starmap Press, Beijing in Chinese

Zhang Z, Zhao X, Wang X (2012b) Altas for remote sensing of land use in China. Starmap Press, Beijing in Chinese

Zheng Y, Qian Y, Miao M, Yu G, Kong Y, Zhang D (2002) The effects of vegetation change on regional climate I: simulation results. ACTA Meteorologica Sinica 60(1):1–16